

# Efficient Multiphysics Analysis of Drum Rollers

Mircea Popescu     David Staton  
Motor Design Ltd.,  
Ellesmere, U.K.

Steven Jennings  
Interroll Trommelmotoren  
GmbH, Wassenberg, Germany

Thomas Barucki  
Adapted Solutions GmbH,  
Chemnitz, Germany

*Abstract* - This paper presents an efficient multiphysics analysis (electromechanics coupled with thermal) of a drum roller that is driven by induction motors. The drum roller performance at variable load can be accurately predicted using a simple non-linear equivalent electric circuit coupled with a customized load profile and a reduced thermal network. The multiphysics analysis is focused on the main problems related to the drum roller operation: stator current variation when a random load level is present and heat extraction via the drum shell and conveyor belt.

The thermal behavior of the induction motor is modeled with a reduced node lumped equivalent thermal network (MotorCAD). Three main sources of heat are considered: stator copper losses, rotor copper losses and stator iron losses. Extra loss components as rotor iron losses or friction losses are included by augmenting the rotor copper losses. The heat extraction in a drum roller is realized mainly via the drum shell and the conveyor belt. The multiphysics analysis is performed in a circuit simulator (PORTUNUS) where the VHDL-AMS electromechanic model is coupled with the thermal network.

## Introduction

The drum motor concept was first produced specifically for conveyor belt applications [1]. The idea is to produce a compact, totally enclosed (IP66) single component drive unit with high efficiency and lower frictional losses than a conventional geared motor. The motor is fixed to a stationary shaft at one end of the drum and directly coupled through the motor's rotor pinion to an in-line helical or planetary gearbox which is fixed to the other stationary shaft. The torque is transferred from the motor via the polymer planetary gearbox to the drum shell made of stainless steel through a coupling or geared rim attached to the shell or end housing (see Figure 1). The design is quick and easy to install, requires no maintenance and because of its totally enclosed hermetically sealed design is not affected by dust, dirt grease or water. There are many examples of the modern day drum motor in airport checks, in conveyors and security machines, supermarket check-outs, food processing conveyors and weighing equipment. Single or 3-phase induction motors are normally used as drum motors. A recent alternative are brushless synchronous permanent magnet motors. All 3 phase motors can be used together with a variable frequency converter drive.



Figure 1: A drum-motor for conveyer roller

## General system

The drum roller system to be analysed consists of

- a three-phase power supply, connected with the electric motor either directly or via a frequency inverter,
- the induction motor having electro-magnetic, thermal and mechanical properties;
- the mechanical load that the drum roller has to overcome.

It is obvious that electromagnetic, thermal and mechanic aspects, all of them coupled by the electric motor model, have to be considered.

The necessary complexity of the sub-models differs. While the mechanic load could be described by relatively simple equations, the electro-magnetic motor model is rather complex due to the consideration of non-linear dependencies like the skin effect and the iron losses. The thermal network of the electric motor is built of several thermal resistances and capacitances. If necessary, it could be expanded easily by means of the schematic editor to account for the heat transfer conditions in the neighbourhood of the motor. The complexity of the electric circuit connected to the electric motor depends on the motor type. For the induction machine (as described in this paper), a simple three-phase voltage source is usually sufficient.

### Electromagnetic model

In equivalent circuits of induction machine [2], for linear modelling, the iron of both stator and rotor is assumed to be of negligible reluctance. A considerable increase in torque output can be achieved for a given machine frame by operating at flux densities for which the iron reluctances are significant in comparison with the air gap reluctance. Among the non-linearities that influence the vector control principles are: iron saturation, iron core losses, rotor resistance and rotor time constant variation. A model that accounts for the saturation and iron losses effects, and suitable for stator flux oriented control, is the  $\Gamma$  model with two inductances, that can be derived directly from the usual no-load and standstill measurements. The flux densities in the teeth and yoke of the stator are dependent primarily on the total stator flux linkage. Similarly, the flux densities in the rotor iron depend primarily on the net rotor flux linkage. The saturation effect is best modelled as a non-linear inductance  $L_{si}$  connected in parallel with the  $\Gamma$  structure of the motor. A stator equivalent core-loss resistance, placed exactly in parallel with stator inductance, is used for modelling compactly core loss phenomena. It was demonstrated that the equivalent core-loss resistance can express appropriately and independently both eddy-current and hysteresis losses, rather than mere vague loss and mere core loss.

In Figure 2 is presented the d-q equivalent circuit for the  $\Gamma$  model of the induction machine in an arbitrarily reference frame. The equivalent circuit may be used for induction motors transient and steady-state operation analysis.

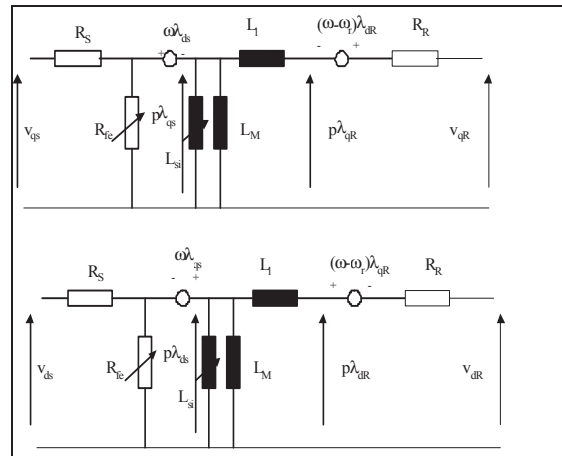


**Figure 2 d-q direct  $\Gamma$  model of the vector controlled induction motor in arbitrarily reference frame**

An induction motor is modelled using voltage and flux equations:

Stator voltage equation:

$$\mathbf{v}_S = \mathbf{i}_S R_S + j\omega_a \lambda_S + p\lambda_S \quad (1)$$

Rotor voltage equation:

$$0 = \mathbf{i}_R R_R + p\lambda_R + j(\omega_a - \omega_r)\lambda_R \quad (2)$$

Stator flux equation:

$$\lambda_S = \left( \frac{L_M L_{si}}{L_M + L_{si}} (\mathbf{i}_M + \mathbf{i}_{si}) \right) \quad (3)$$

Rotor flux equation:

$$\lambda_R = L_L \mathbf{i}_R + \lambda_S \quad (4)$$

Mechanical equation:

$$T_e - T_L = J_m p \omega_r + B_m \omega_r \quad (5)$$

$$T_e = \frac{3P}{4} \operatorname{Re} \left( \lambda_S \cdot (\mathbf{i}_S - \mathbf{i}_{fe})^* \right) \quad (6)$$

Where  $\mathbf{y} = y_q + j \cdot y_d$  is used to denote state variable: voltages, currents, fluxes.

When rotor flux is chosen to implement a sensorless vector control system, the most suitable equivalent circuit for implementing the induction motor model is the inverse  $\Gamma$  model. The effect of stator saturation and core loss can be included in the inverse  $\Gamma$  model of equivalent circuit by connecting:

- the non-linear inductance  $L_{si}$  in parallel with the voltage produced by the time rate of change of stator flux linkage;
- The non-linear resistance  $R_{fe}$  function of the stator frequency and the flux densities in the stator yoke and teeth in parallel with the stator inductance.

In Figure 3 is presented the equivalent circuit for the  $d$ - $q$  inverse  $\Gamma$  model of the induction machine in an arbitrarily reference frame. This model may be used for induction motors transient and steady-state operation analysis.

The voltage and flux equations are as follows:

Stator voltage equation:

$$\mathbf{v}_S = \mathbf{i}_S R_S + j \omega_a \lambda_S + p \lambda_S \quad (7)$$

Rotor voltage equation:

$$0 = \mathbf{i}_R R_R + p \lambda_R + j(\omega_a - \omega_r) \lambda_R \quad (8)$$

Stator flux equation:

$$\lambda_S = L_{si} \mathbf{i}_{si} = L'_L (\mathbf{i}_S - \mathbf{i}_{fe} - \mathbf{i}_{si}) + \lambda_R \quad (9)$$

Rotor flux equation:

$$\lambda_R = L'_M \mathbf{i}_M \quad (10)$$

Mechanical equation:

$$T_e - T_L = J_m p \omega_r + B_m \omega_r \quad (11)$$

$$T_e = \frac{3P}{4} \cdot \operatorname{Re} \left( \lambda_R \cdot (\mathbf{i}_S - \mathbf{i}_{fe})^* \right) \quad (12)$$

where  $\mathbf{y} = y_q + j \cdot y_d$  is used to denote state variable: voltages, currents, fluxes.

The equation systems of direct and inverse  $\Gamma$  models of the induction motor can be implemented in PORTUNUS using VHDL-AMS language. The non-linear elements of the equivalent circuit:

- inductance  $L_M$ , stator and rotor resistance and equivalent resistance  $R_{fe}$  have been implemented by considering their variation with load, frequency and temperature.  $R_{fe}$  can be determined from no-load measurements.

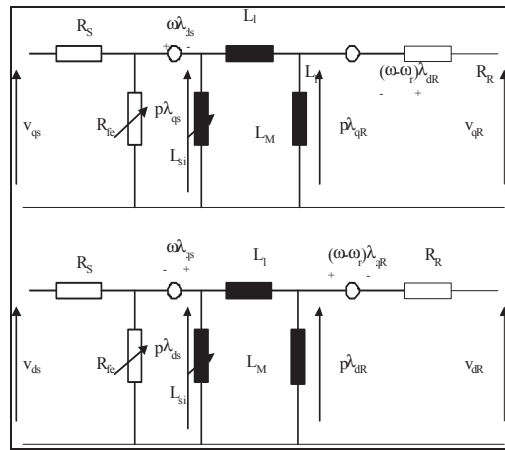


**Figure. 3 d-q inverse  $\Gamma$  model of the vector controlled induction motor in arbitrarily reference frame**

- Magnetizing inductance is modelled as a function of the magnetizing current. The coefficients  $L_0$ ,  $L_1$ ,  $L_2$  can be determined either experimentally via a no-load test or by computation using an analytical (SPEED software module - PC-IMD) or numerical program (FLUX2D).

$$L_m = L_0 + L_1 |\mathbf{i}_m| + L_2 (|\mathbf{i}_m|)^2 \quad (13)$$

- Stator and rotor resistance values include the temperature effect.
- Rotor resistance value includes the skin-effect via the formula:

$$R_{2ac} = R_{2dc} K_r \quad (14)$$

$$K_r = \xi \frac{(\sinh 2\xi + \sin 2\xi)}{(\cosh 2\xi - \cos 2\xi)}$$

$$\xi = h_s \sqrt{\frac{s \omega_l \mu_0 \sigma_{Al}}{2}}$$

### Thermal model

The lumped thermal network used to model the induction motor thermal behaviour is obtained from Motor-CAD [4]. In Figure 4 and Figure 5, the temperature distribution in motor cross-section and in axial direction respectively is displayed.

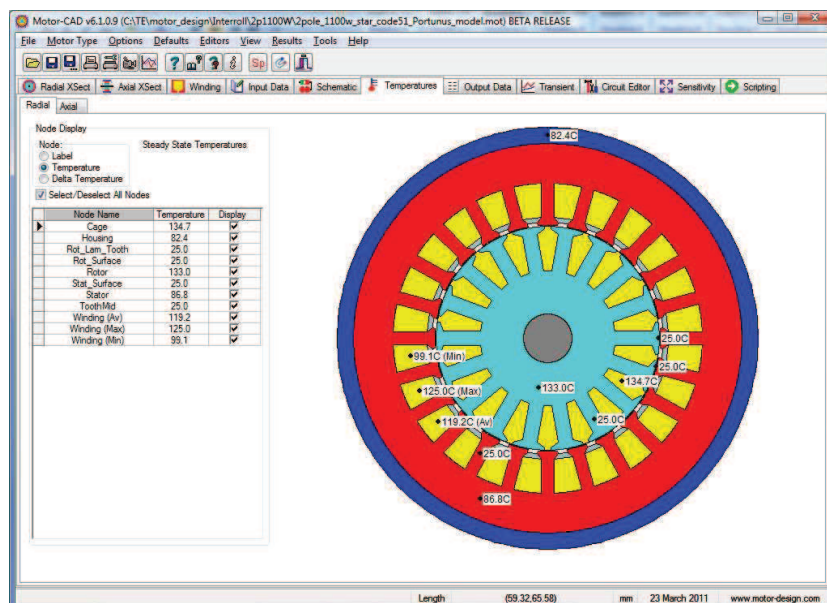


**Figure 4 Cross-section of an induction motor in Motor-CAD**

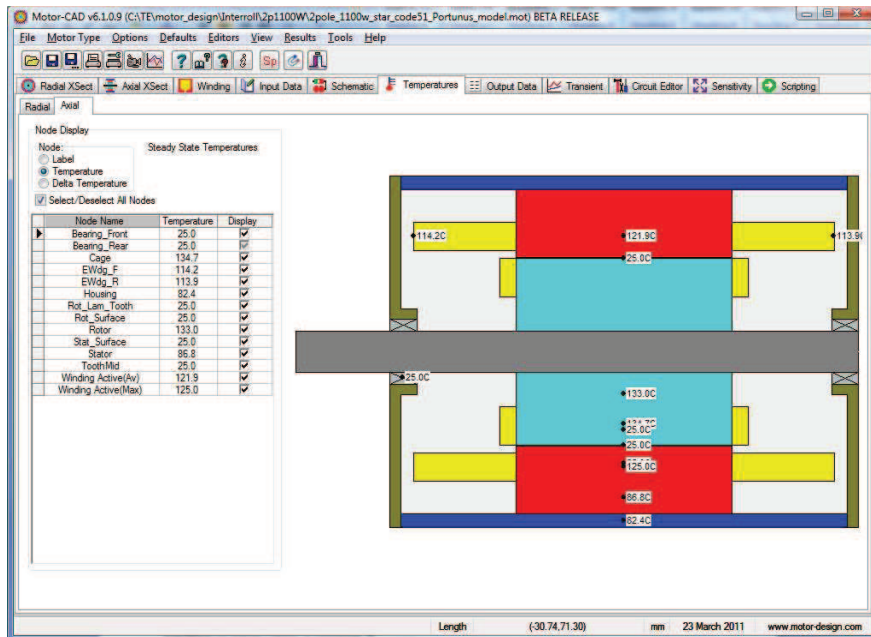


Figure 5. Axial view of an induction motor in Motor-CAD

MotorCAD will calculate a reduced thermal network with just 8 nodes.

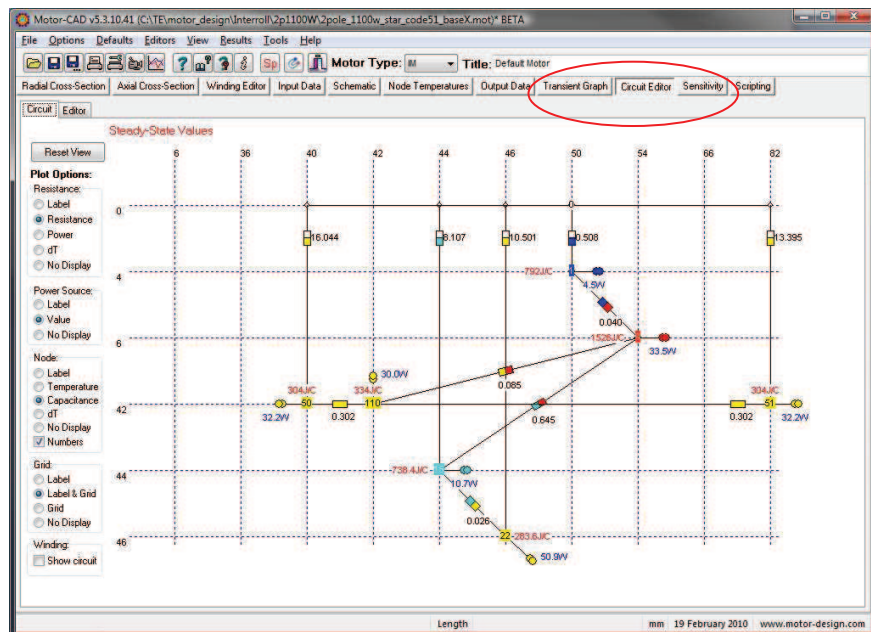


Figure 6 Reduced thermal network in Motor-CAD

This circuit will be further imported by PORTUNUS to define the thermal behaviour of the induction motor.

This circuit needs to be further modified, by eliminating the stator winding losses, rotor cage losses and stator iron loss sources with inputs from the electro-mechanic VHDL-AMS model.

Also end-winding copper loss sources are deleted as the electro-mechanic model does not calculate these values. The housing loss source is maintained with the constant value coming from Motor-CAD. Some further changes become necessary if the model shall be used by a script and a proper handling of initial values is required.

Experiments demonstrated that it is recommended that the template induction motor thermal model is used for the analysis of any existing motor and changing the values of the thermal resistances and thermal capacitances as calculated by Motor-CAD.

## Mechanical model

The mechanical part of the motor is modeled by a customized variation law. The load is characterized by a combination of a constant torque and a speed-dependent torque with exponential characteristic, the sign of both being dependant on the direction of the rotation

## Implementation

The system has been modelled in the simulation software PORTUNUS [5]

The electro-magnetic model of the motor has been implemented by using the standardized modelling language VHDL-AMS [6] which makes it quite easy to translate the equation set of the machine into model text. Figure 7 (showing the equations for the rotor voltages) demonstrate the seamless transformation.

Beside the easy implementation of the equation set, the ability of VHDL-AMS to handle so-called “architectures” has been interesting for the projects. This means that several equations sets can be provided for a model. In our case, the “direct  $\Gamma$ ” and “inverse  $\Gamma$ ” induction motor models have been implemented [2]. The VHDL-AMS model describing the electro-magnetic behaviour of the motor can be used for the transient simulation and the operating point analysis.

$$0 = R_r * K_r * (1 + \alpha_r * (T_r - 293)) * i_{2d} - \frac{d\Psi_{2d}}{dt} + \omega_e * \Psi_{2q}$$

$$0 = R_r * K_r * (1 + \alpha_r * (T_r - 293)) * i_{2q} + \frac{d\Psi_{2q}}{dt} - \omega_e * \Psi_{2d}$$

VHDL-AMS:

$$0.0 == R_r * K_r * (1.0 + Alpha_r * (T_rotor - 293.15)) * i2d + Psi2d'dot + w_e * Psi2q;$$

$$0.0 == R_r * K_r * (1.0 + Alpha_r * (T_rotor - 293.15)) * i2q + Psi2q'dot - w_e * Psi2d;$$

**Figure 7 Example of model equations and VHDL-AMS text**

A thermal equivalent network has been used for the modelling of the thermal behaviour of the motor. It uses the same structure as it is produces by Motor-CAD when it exports data to PORTUNUS.

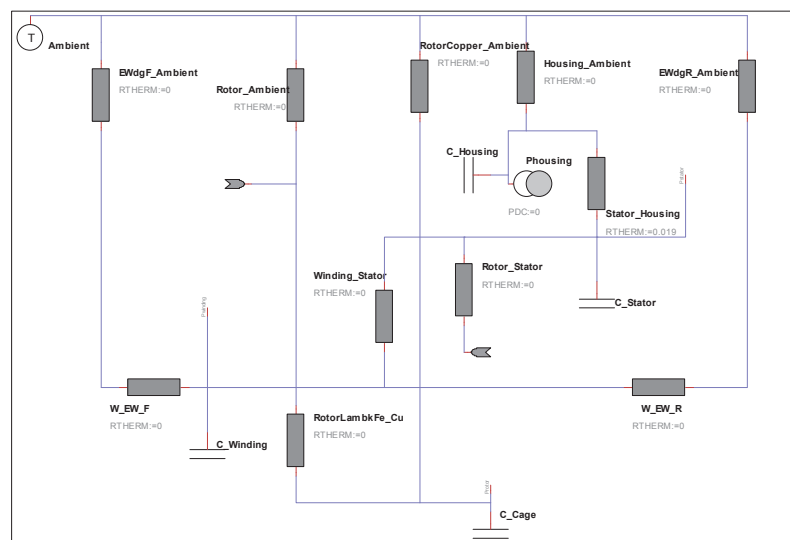


**Figure 8 Thermal network for the induction motor**

Figure 8 shows the structure of the thermal network. It features three terminals that provide the simulation interface to the VHDL-AMS model of the motor described above. The VHDL-AMS

model forces a heat flow into the thermal network and may read the resulting temperatures which in turns have an influence on the motor losses.

Since the models of the thermal network are placed into the PORTUNUS schematic as graphical objects, the network can be easily expanded to take into account for the thermal conditions at the adjacent parts. The thermal model of the motor can be used for transient simulations as well as operating point and DC calculations. For the DC (steady-state) analysis, the differential equation terms introduced by the thermal capacitances are ignored by the simulator.

The model of the mechanical part is again implemented using VHDL-AMS. While the motor inertia is part of the motor model, the load is represented by a second VHDL-AMS model.

In the case of an induction machine drive, the electrical network consists of the three-phase voltage source (PORTUNUS model) only.

Figure 9 shows the system model structure at the top level schematic.

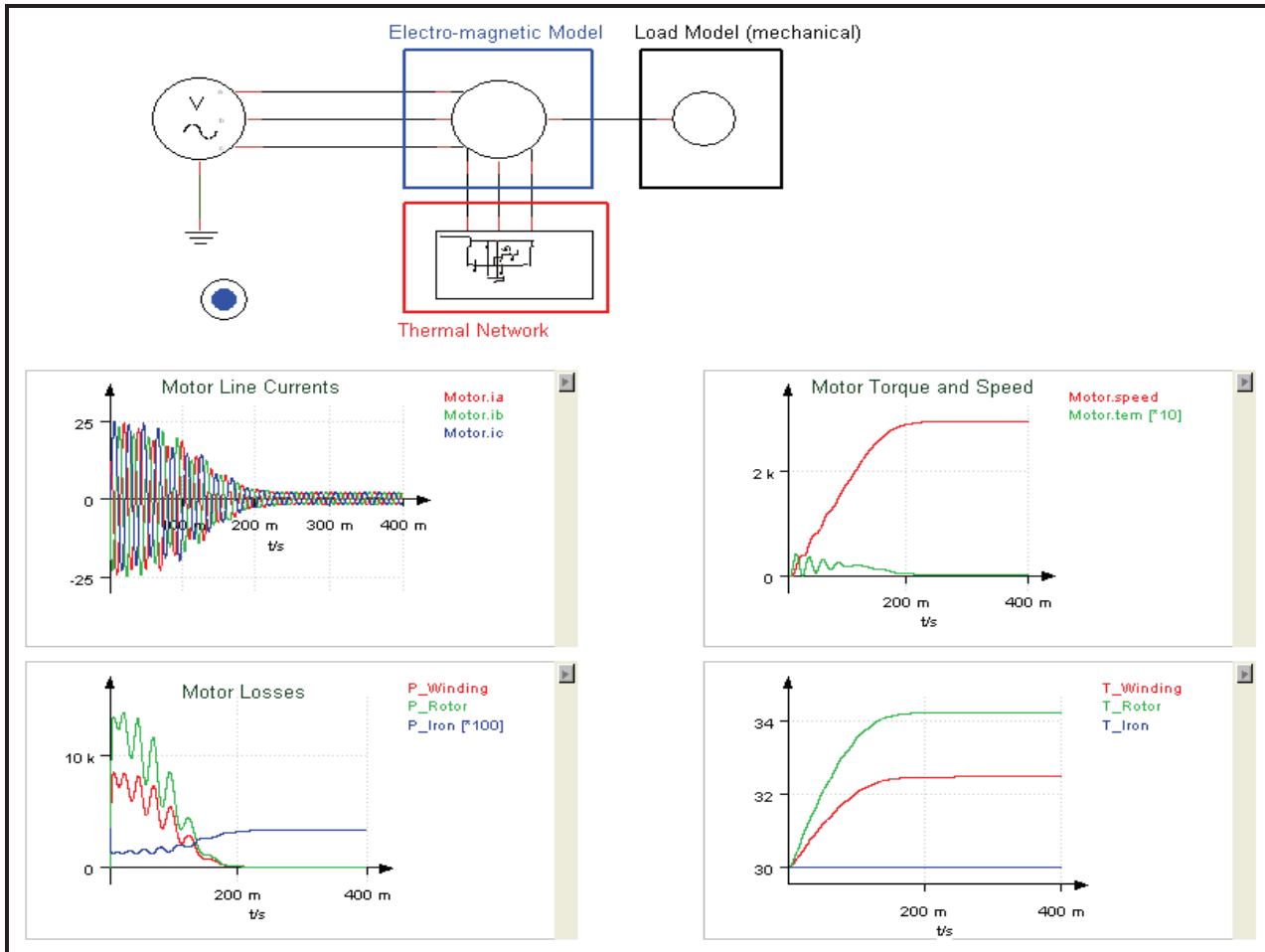


Figure 9 Multiphysics schematic of the drum roller model

### Experimental data validation

Figures 10 to 12 show a comparison between test data and computed values for a 2-pole, 2.2kW induction motor for drum roller. Figure 13 shows a typical thermal image of a motor under test.

Note a satisfactory agreement between experiments and calculations for speed and current versus torque variations, Figure 10 and Figure 12 respectively. The calculated total losses are higher than the measured values. This is correlated to the slightly higher calculated values for the stator current, which translates into higher stator copper losses, but can be also associated with a difference in power factor values due to reactance variation with current that is difficult to estimate. Measured steady-state winding temperature is 138 °C as compared to 145 °C calculated value.

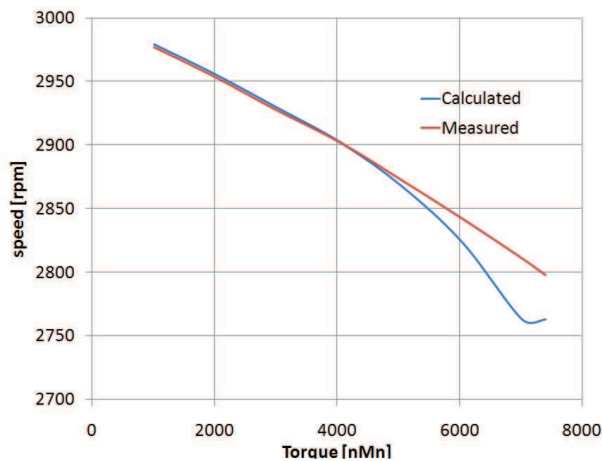


Figure 10: Speed vs torque

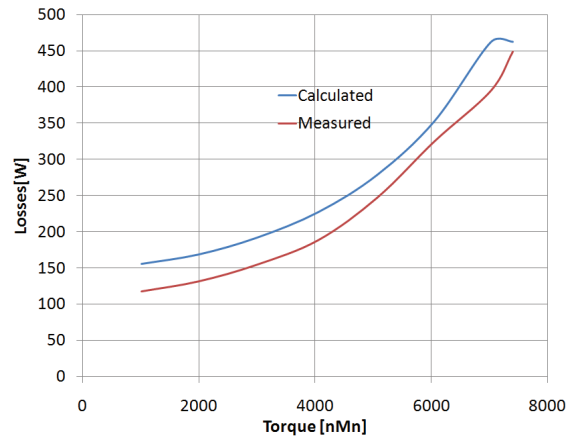


Figure 11 Losses vs torque

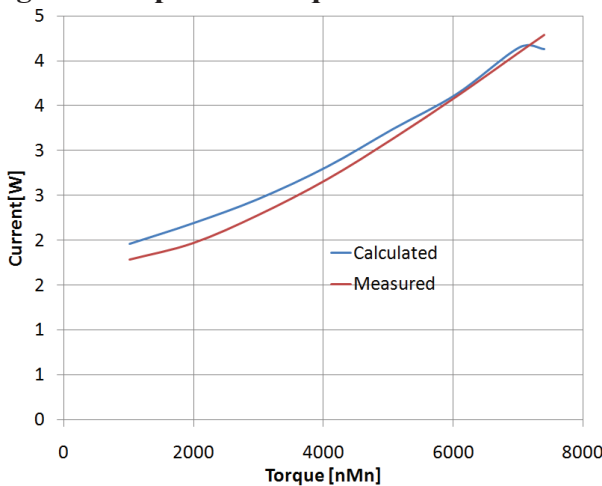


Figure 12: Current vs torque

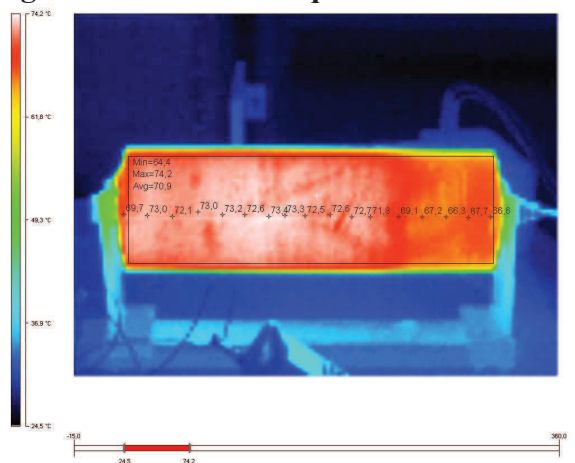


Figure 13 Thermal image for drum roller motor

## Conclusions

An efficient multiphysics analysis of a drum roller system is proposed. Non-linear phenomena like saturation and resistance variation with temperature and skin-effect are included in the model. The equivalent circuit parameters are extracted from standard tests, i.e. no-load and locked-rotor tests. The determination of the model parameters describing the heat transfer conditions has been done in the software Motor-CAD which may automatically export the resulting equivalent circuits into PORTUNUS.

The fast determination of steady-state conditions can be done with the help of a script that controls a sequence of transient simulations and DC calculations both running in PORTUNUS. This script has been implemented using Excel and VBA.

## References

- [1] E. Drexler, "Conveyer Roller", US Patent # 1,889,173, 1932
- [2] G.R. Slemon, "Modelling of induction machines for electric drives", *IEEE Transactions on Ind. Appl.*, Vol. 25,(6), Nov/Dec. 1989, pp. 1126-1131
- [3] D. Staton, A. Boglietti, A. Cavagnino, "Solving the More Difficult Aspects of Electric Motor Thermal Analysis, in small and medium size industrial induction motors", *IEEE Transaction on Energy Conversion*, Vol.20 (3) pp.620-628.
- [4] [www.motor-design.com](http://www.motor-design.com)
- [5] [www.adapted-solutions.com](http://www.adapted-solutions.com)
- [6] IEEE Standard VHDL Analog and Mixed-Signal Extensions. IEEE, 1999